A 1D coordination network built from trimeric Co(II) units: Synthesis, characterisation and gas sorption properties☆

Emma Regincós Martí [a], Jay McCarron [a,1], Beatriz Doñagueda Suso [a], Alan R. Kennedy [a], Ashleigh J. Fletcher [b], Gavin A. Craig [a,*]

[a] Department of Pure and Applied Chemistry, University of Strathclyde, Glasgow G1 1RX, United Kingdom
[b] Department of Chemical and Process Engineering, University of Strathclyde, Glasgow G1 1XW, United Kingdom

ARTICLE INFO

ABSTRACT

Ligands based on bicyclo[2.2.2]oct-7-ene units have been used previously to obtain porous metal–organic materials, including 3D frameworks, 2D sheets, and discrete porous cages. The steric bulk of this unit helps to generate porosity in these materials, and so it has also been incorporated into porous organic cages for this purpose. In this contribution, we describe a new, nitro-functionalised ligand, **LH₂**, containing this unit, which yields a 1D coordination network, **1**, upon reaction with cobalt(II) acetate. The ligand itself is found to crystallise readily, and we describe its crystal structure and gas sorption measurements for uptake of N_2. The coordination network **1** consists of linear, trinuclear Co(II) metal nodes that are bridged by pairs of ligands to create an intrinsic pore that is occupied by coordinated dimethylacetamide molecules (DMA). Solvent exchange and activation experiments were unsuccessful in removing DMA, but the orientation of the nitro-groups of the polymer into the space between the chains motivated CO_2 sorption studies at room temperature, reaching nearly 0.5 mmol/g at 20 bar of absolute pressure.

1. Introduction

Porous coordination polymers, or metal–organic frameworks (PCPs or MOFs, respectively), are widely studied materials thanks to their range of potential applications in, for example, catalysis [1,2], drug delivery [3,4], sensing [5,6], gas capture [7,8] and separation [9,10]. These applications arise from the architecture of the framework or polymer; the pore structure; the functionalisation of the ligands; and other properties that can originate in the metal centres such as magnetism or catalysis through open metal sites. A key development in these materials has been the use of design principles to target specific network topologies. These have been described in terms that consider matching the likely coordination geometry around a transition metal ion with the symmetry of the ligand, as exemplified by the targeted synthesis of the diamond-like network $[Cu[C(C_6H_4CN)_4]^+{}_n$ by Robson at the end of the 1980s [11–13]. The development of more complex, polynuclear metal nodes, known as secondary building units (SBUs), then proved to be pivotal in the field both in terms of the accessible architectures and the

potential applications of the materials [14,15].

Regardless of whether the metal nodes in a MOF or PCP are formed by single metal ions or SBUs, the most basic characteristic of these materials is the dimensionality of the coordination network. 3D and 2D networks, as suggested by their name, contain coordinate and covalent bonds in 3 or 2 dimensions, respectively, with the latter sometimes referred to as metal–organic nanosheets (MONs) [16]. Following the terminology recommended by IUPAC, one of the conditions for considering a 1D coordination polymer to be a coordination network is if an individual polymer within the material contains loops [17]. Herein, we describe the synthesis of a new ligand derived from bicyclo[2.2.2] oct-7-ene-2,3,5,6-tetracarboxylic dianhydride, and its use to obtain a 1D coordination network containing a linear $[Co_3]$ motif as metal node. The interest in this bulky bicyclo[2.2.2]oct-7-ene unit is that it can help retain porosity, an approach that has been used by incorporating this moiety into porous organic cages [18]. The dianhydride can be reacted with amino-benzoic acid derivatives to give multi-dentate carboxylic acid ligands, which are favourable for the synthesis of metal–organic

---

materials [19]. Using this approach, tetra-carboxylic acid derivatives, where the carboxylic acid groups are both in the *meta-* position relative to the dicarboxiimide, have been used to obtain 3D networks for capture of uranyl ions and tunable luminescence in Ln-based MOFs [20,21]. Dicarboxylic acid derivatives, where the carboxylic acid is found in the *para-* position relative to the dicarboxiimide, have been used to obtain 2D sheets [22]. Recently, we found that when the dicarboxylic acid derivatives have the carboxylic acid groups *meta-* to the dicarboxiimide then they can be used to obtain permanently porous lantern-type cages, *i.e.* 0D assemblies based on [Cu$_2$] paddlewheels [23,24]. In this paper, we describe a new ligand which retains the carboxylic acid in the *meta-* position, but we have additionally functionalised the benzoic acid rings with an –NO$_2$ group in the *para-* position (**LH$_2$**; Fig. 1 and Fig. S1). Finding that **LH$_2$** crystallises readily, we report its crystal structure and attempts to measure its gas uptake. Reaction of **LH$_2$** with cobalt acetate yielded a 1D coordination network in which pairs of L^{2-} ligands bridge between linear [Co$_3$] nodes to form the coordination polymer [Co$_3$(L)$_2$(OAc)$_2$(DMA)$_2$]$_n$, (**1**). Although it was not possible to remove the solvent from the crystal structure to maximise the potential porosity of the material, we found that it presents modest porosity towards CO$_2$ at high temperature, which we attribute to uptake of the gas in the space between the polymer chains.

2. Experimental section

2.1. Synthesis

All reagents were used as purchased without further purification.

LH$_2$: 5-amino-2-nitrobenzoic acid (1.994 g, 10.95 mmol) and bicyclo [2.2.2]oct-7-ene-2,3,5,6-tetracarboxylic dianhydride (1.360 g, 5.48 mmol) were suspended in acetic acid (60 mL) and the resulting off-white suspension was refluxed at 115 °C for 48 h, forming a cream suspension. After cooling to room temperature, the solids were collected by vacuum filtration and washed with ethanol (3 × 10 mL) to give an off-white powder. Yield: 83 %. Crystals suitable for single-crystal X-ray diffraction were obtained by slow evaporation of the mother liquor, in which the compound is present as the trihydrate **LH$_2$·3H$_2$O**. ^{1}H NMR (DMSO-d_6, 400 MHz, 25 °C) δ (ppm): 14.15 (COOH, s, 1.1H), 8.14 (C$_6$H$_3$, d, 2H, J = 8.6 Hz), 7.70 (C$_6$H$_3$, d, 2H, J = 2.2 Hz), 7.62 (C$_6$H$_3$, dd, 2H, J = 8.6, 2.2 Hz), 6.36 (CH = CH, dd, 2H, J = 3.1 Hz, 4.1 Hz), 3.57 (CH, s, 2H), 3.51 (CH, s, 4H). ^{13}C NMR (DMSO-d_6, 400 MHz, 25 °C) δ (ppm): 176.6, 165.5, 147.7, 136.0, 131.7, 130.7, 128.6, 128.1, 125.4, 43.1, 34.4. See Fig. S2. IR: 1727 cm^{-1}, C=O stretching (dicarboxiimide ring); 1701 cm^{-1}, C=O stretching (carboxylic groups); 1547 cm^{-1}, C=C

stretch; 1365 cm^{-1}, C—C stretch, aromatic ring; 883 cm^{-1}, =C—H bend; 753 cm^{-1}, C—H bending (substituted aromatic ring); 699 cm^{-1}, C—H bending (substituted aromatic ring), Fig. S3. Elemental analysis calculated for **LH$_2$** (C$_{26}$H$_{16}$N$_4$O$_{12}$·0.5H$_2$O): C, 53.34; H, 2.93; N, 9.57 %. Found: C, 53.58; H, 2.93; N, 9.49 %.

[Co$_3$(L)$_2$(OAc)$_2$(DMA)$_2$]$_n$, (**1**): A solution of **LH$_2$** (120 mg, 0.21 mmol) in 1 mL of dimethylacetamide (DMA) was added to a thin suspension of Co(OAc)$_2$·4H$_2$O (51 mg, 0.21 mmol) in DMA (2 mL), yielding a thin, purple suspension. The vial was placed in the oven for 3 days at 100 °C, and when it was removed from the oven contained 98 mg of dark purple crystals suitable for single crystal X-ray diffraction (Table S1). Yield: 57.8 %. Acid digestion ^{1}H NMR (DMSO-d_6, DCl, 400 MHz, 25 °C) δ (ppm): 8.14 (C$_6$H$_3$, d, 2H, J = 8.6 Hz), 7.70 (C$_6$H$_3$, d, 2H, J = 1.6 Hz), 7.62 (C$_6$H$_3$, dd, 2H, J = 7.0, 1.6 Hz), 6.35 (CH = CH, t, 2H, J = 3.4 Hz), 3.56 (CH, s, 2H), 3.51 (CH, s, 4H), 2.95 (CH_3COCN(CH_3)$_2$, s, 3H), 2.79 (CH_3COCN(CH_3)$_2$, s, 3H), 1.97 (CH_3COCN(CH$_3$)$_2$, s, 3H), 1.91 (CH_3COO$^-$, s, 3H), Fig. S4 IR: 1722 cm^{-1}, C=O stretching (dicarboxiimide ring); 1539 cm^{-1}, C=C stretch; 1378 cm^{-1}, C—C stretch, aromatic ring; 1376 cm^{-1}, C—C stretch; 853 cm^{-1}, =C—H bend; 745 cm^{-1}, C—H bending (substituted aromatic ring); 698 cm^{-1} C-H bending (substituted aromatic ring); Fig. S5. Elemental analysis calculated for 1 (Co$_3$C$_{64}$H$_{52}$N$_{10}$O$_{30}$): C, 47.51; H, 3.24; N, 8.66 %. Found: C, 47.19; H, 3.53; N, 8.72 %.

[Co$_3$(L)$_2$(OAc)$_2$(DMA)$_2$]$_n$ – Solvent Exchange (**1-SE**): Crystals of **1** were submerged in acetone and the solvent was exchanged 7 times.

2.2. Physical characterisation

NMR data were collected at room temperature on a Bruker AVANCE 400 NMR spectrometer, operating at 400.13 MHz for ^{1}H and 100.62 MHz for ^{13}C. Acid digestion experiments were performed by suspending ca. 10 mg of complex in DMSO-d_6 and adding 20 μL of DCl solution. Elemental analyses were collected using a Thermo Scientific FlashSmart CHNS Elemental Analyzer in the Department of Civil and Environmental Engineering at the University of Strathclyde. Powder X-Ray Diffraction (PXRD) data were collected at room temperature, on a flat plate, using a poly(methyl methacrylate) holder. The instrument used was a Bruker D8 Discover in a $\theta/2\theta$ Bragg-Brentano reflection geometry using a Cu K$_\alpha$ source (λ = 1.54056 Å), available within the Centre for Continuous Manufacturing and Advanced Crystallisation (CMAC), at the University of Strathclyde. Fourier-Transform infra-red spectra were collected using a NICOLET iS5 Thermo Scientific spectrometer, with parameters set as 48 scans and a resolution of 4 cm^{-1}. Thermogravimetric analyses of the samples were performed with a NETZSCH STA 449 F1 Jupiter under N$_2$ in the Department of Chemical and Process Engineering at the University of Strathclyde. The sample was heated to 500 °C at a rate of 10 °C/min. Disposable Aluminium pans were used as holders for the samples. Nitrogen adsorption measurements were undertaken at −196 °C using a Micrometrics ASAP 2420, in the Department of Chemical and Process Engineering, at the University of Strathclyde. Surface areas were calculated using the Micromeritics software MicroActive 5.02. CO$_2$ sorption measurements were performed with the Hiden Isochema Ltd. Intelligent Gravimetric Analyser, IGA-003. Prior to the measurement the sample was degassed by heating at 30 °C under vacuum. The mass uptake was measured and the maximum time for equilibration at any given pressure was 3 h, with the temperature maintained constant using a water bath.

2.3. Single crystal X-Ray diffraction

All crystallographic measurements were made with monochromatic Cu radiation (λ = 1.54184 Å) using an Oxford Diffraction Gemini-S diffractometer. Raw data processing used the program CrysalisPro [25]. The structures were solved using direct methods and were refined against F^2 to convergence using all unique reflections and the program Shelxl [26], as implemented within WinGX [27]. For compound **LH$_2$** two
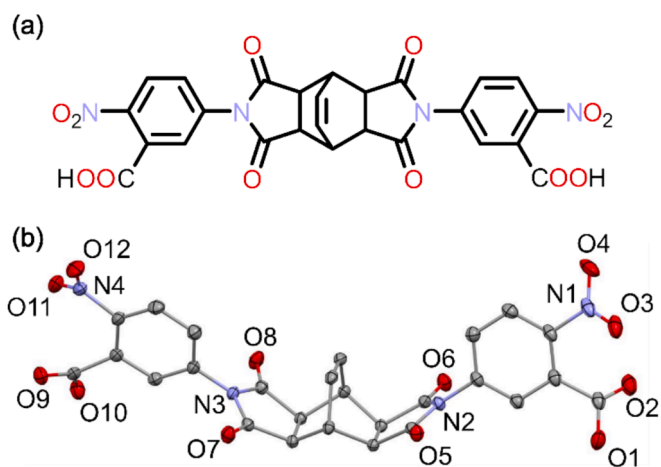

Fig. 1. a) Structure of the ligand **LH$_2$**. b) View of the crystal structure of the molecule **LH$_2$**, with hydrogen atoms omitted for clarity and ellipsoids shown at the 50% probability level.

of the three independent water sites were modelled as disordered. For compound **1** the DMA solvent and the MeCOO⁻ anion are disordered about symmetry operators. The nitrobenzoate ring of the ligand was also modelled as disordered over two sites – appropriate restraints and constraints were added to ensure that each approximated to normal geometry and displacement behaviour. Selected crystallographic and refinement parameters are given in Table S1 and full information in .cif format has been deposited with the CCDC, as reference numbers 2378507 and 2378508.

3. Results and discussion

In recent work, we have used ligands containing the bicyclo[2.2.2] oct-7-ene unit as a means of obtaining coordination cages that show gas uptake. Having found that this gas uptake could be tuned depending on the functional groups attached to the benzoic acid groups of the ligand, here we continued this work by synthesising a new ligand with a nitro-functionalised benzoic acid ring (**LH₂**). **LH₂** was obtained in good yields by refluxing 5-amino-2-nitrobenzoic acid with bicyclo[2.2.2]oct-7-ene-2,3,5,6-tetracarboxylic dianhydride in acetic acid (Fig. S1). The synthesised ligand was obtained both as a bulk powder and as crystals suitable for single crystal X-ray diffraction. The product was analysed by powder X-ray diffraction (PXRD), and the obtained diffractogram matched well with the one predicted from single-crystal data, which confirms the phase purity of the product (Fig. 2(a)). Analysis of the single crystal diffraction data show that the ligand crystallises in the monoclinic space group $P2_1/c$ (Table S1). The asymmetric unit contains one ligand molecule, and three water molecules with occupancies that are split over five positions. There is some disorder present around the nitro groups due to their free rotation. The ligand packs efficiently through stacks of planes of **LH₂** – three layers of these planes are shown in Fig. 2(b). The interactions between the layers are driven by strong hydrogen bonding that involves the carbonyl groups of the dicarboximide rings, the carboxylic acid groups, and the nitro groups (Fig. S6). The view along the *a*-axis shows the channels parallel to this crystallographic dimension, which could favour porosity in the material (Fig. 2 (c)).

Reaction of **LH₂** with cobalt(II) acetate in DMA yielded single crystals directly from a one-pot reaction. The resulting product is a one-dimensional coordination polymer with the formula $[Co_3(L)_2(OAc)_2(DMA)_2]_n$, **1**, that crystallises in the monoclinic space group $C2/m$. The asymmetric unit consists of one quarter of the formula

unit (Fig. 3). Through charge balance considerations, all of the cobalt ions in the structure are assigned as Co(II). These ions are arranged in a linear trimeric unit, with Co1 and its symmetry equivalent Co1′ in the outer positions, and Co2 in the central position (Fig. 4(a), and metric parameters in Table 1). Co1 is found in a tetrahedral coordination environment, coordinated by four donor oxygen atoms. One of these is from a terminal DMA molecule; two are from the carboxylate groups of two different L^{2-} ligands, which both bridge to Co2; and one is from an acetate anion that bridges to Co2. This leads to a distance between Co1 and Co2 of 3.651(1) Å. The distortion around the Co(II) ions was measured using the program Shape 2.0 [28,29]. Shape provides a continuous shape measure, *S*, indicating how close the coordination sphere of a central atom resembles ideal reference polyhedra, where ideal symmetry is associated with $S = 0$. When more than one geometry is possible for a given coordination sphere, lower values of *S* indicate the best approximation. For Co1, $S_{tet} = 7.6$, $S_{see-saw} = 11.8$, and $S_{square\ planar} = 27.1$. This shows that while the coordination environment of Co1 is best-described by a tetrahedron, there is a slight distortion towards a see-saw geometry, associated with C_{4v} symmetry. Co2 is coordinated by six oxygen atoms in a distorted octahedron, one for each of the two acetate bridges and four from four different L^{2-} ligands (Fig. 4(a)). Shape measures here found that this coordination environment of Co2
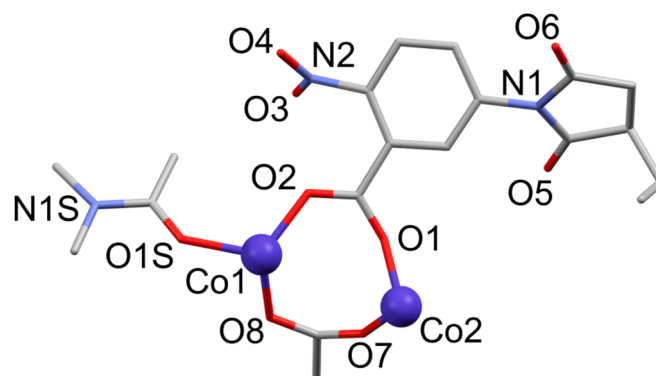
Fig. 3. View of the asymmetric unit of **1**. Colour code: Co, purple; O, red; N, blue; C, grey. Hydrogen atoms and minority disordered components omitted for clarity. (For interpretation of the references to colour in this figure legend, the reader is referred to the web version of this article.)
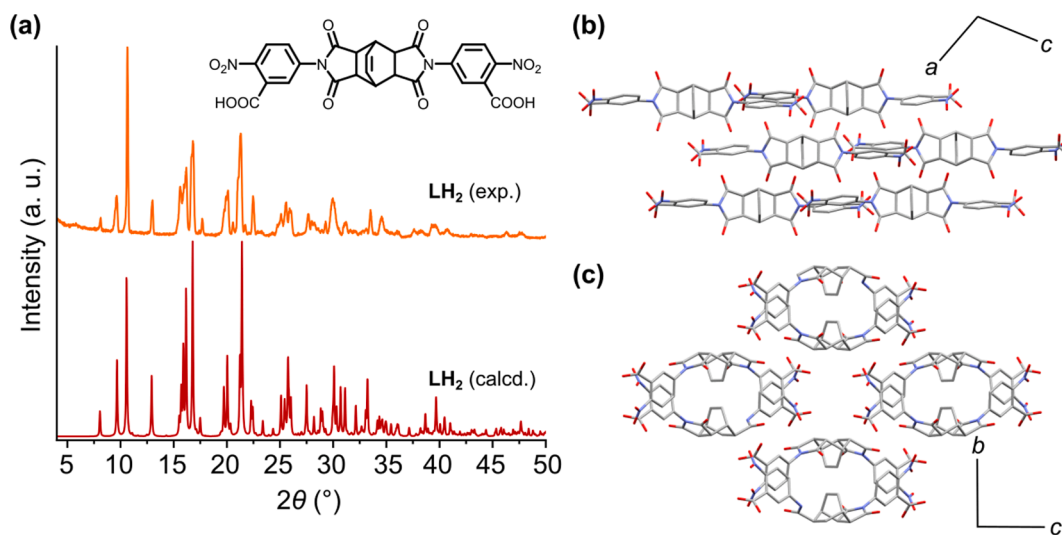
Fig. 2. a) PXRD data calculated for the structure from single crystal (bottom, red) and experimental data from bulk powder (top, orange) of **LH₂** with inset showing the molecular structure; b) view along the *b*-axis; c) view along the *a*-axis. Colour code: O, red; N, blue; C, grey. Hydrogen atoms and water molecules are omitted for clarity. (For interpretation of the references to colour in this figure legend, the reader is referred to the web version of this article.)
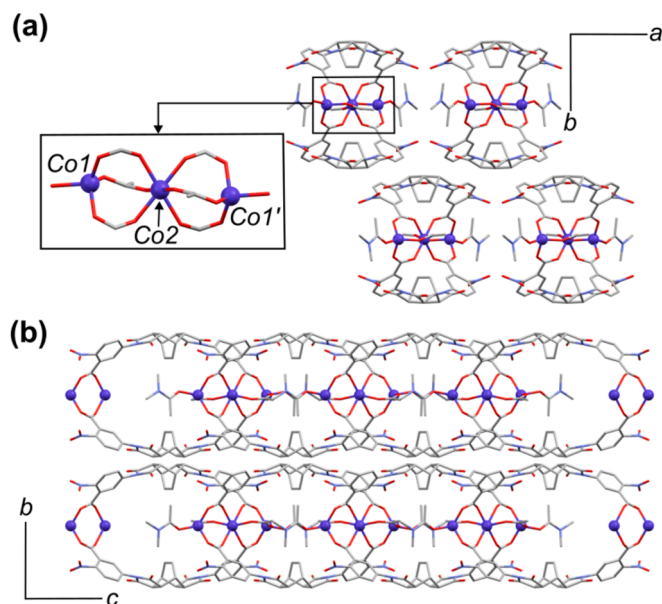
Fig. 4. Different views of the crystal structure of **1**: a) front view of the chains along the *c*-axis, with detail of the trimeric unit and coordination sphere of the Co(II) ions. b) Side view of the chains along the *c*-axis. Colour code: Co, purple; O, red; N, blue; C, grey. Hydrogen atoms omitted for clarity. (For interpretation of the references to colour in this figure legend, the reader is referred to the web version of this article.)

Table 1
Selected Bond Lengths and angles for complex **1**.

Bond	Length/Å
Co1-O2	1.879(16)
Co1-O1S	1.978(5)
Co1-O8	1.942(8)
Co2-O1	2.075(6)
Co2-O7	2.031(7)

Atoms	Angle/°
O2[1]-Co1-O2	111.3(11)
O2[1]-Co1-O1S	98.4(4)
O2-Co1-O1S	114.5(3)
O2-Co1-O8	118(2)
O2[1]-Co1-O8	113(2)
O8-Co1-O1S	100.4(4)
O7-Co2-O1	70.6(3)
O7-Co2-O1[1]	88.2(3)
O7-Co2-O1[2]	91.8(3)
O7-Co2-O1[3]	109.4(3)
O1-Co2-O1[1]	111.0(4)
O1-Co2-O1[2]	69.0(4)
O1-Co2-O1[3]	180.0(2)
O1[1]-Co2-O1[2]	180.0(2)

[1] $+X,-Y,+Z$.
[2] $2-X,+Y,1-Z$.
[3] $2-X,-Y,1-Z$.

was best described as a distorted octahedron, rather than a trigonal prism ($S_{oct} = 7.0$ *vs.* $S_{trig.\ prism} = 16.2$). The configuration of a linear trimer of metal ions with coordination numbers 4–6-4 has been reported previously, particularly for trimeric units containing $[Zn(II)_3]$ [30–36]. For $[Co(II)_3]$ it has been reported seven times, but only for discrete molecules rather than for polymers (Table S2). When viewed along the *c*-axis, these polymers present a height that is comparable to their width (11 Å × 10 Å), giving them an overall cylindrical form (Fig. 4(a)). A pair of the L^{2-} ligands bridge from one trimeric unit to the next, leading to the formation of the one-dimensional polymers that run parallel to the *c*-

axis of the unit cell, and creating an approximately oval-shaped cavity (Fig. 4(b)). The bridging acetate groups sit within these cavities. As can be seen in Fig. 4(b), the nitro groups on the ligand point into the interstitial space between neighbouring polymers. PXRD was obtained to confirm phase purity, and the diffractogram is in good agreement with the one predicted from the single-crystal data (Fig. 5(a) and S7).

Thermogravimetric analysis (TGA) of crystalline **LH₂** showed an initial mass loss of 12.7 %, between room temperature and *ca.* 140 °C, related to the loss of the water from within the structure (Fig. 5(b)). This loss is followed by a plateau until 364 °C whereupon a two-step degradation process starts. The TG profile of **1** shows a slight weight loss until the onset of decomposition at *ca.* 320 °C. There are no clear steps that could be related to the loss of the coordinated DMA molecule or solvent release.

In porous molecular solids, porosity can arise from awkward packing of the molecules, or through the formation of regular pores induced by hydrogen bonding motifs, such as those found in hydrogen-bonded organic frameworks [37–39]. Given the channels observed in the crystal structure of **LH₂**, and the potential for awkward packing and porosity generated by the bicyclo[2.2.2]oct-7-ene units, we measured its uptake
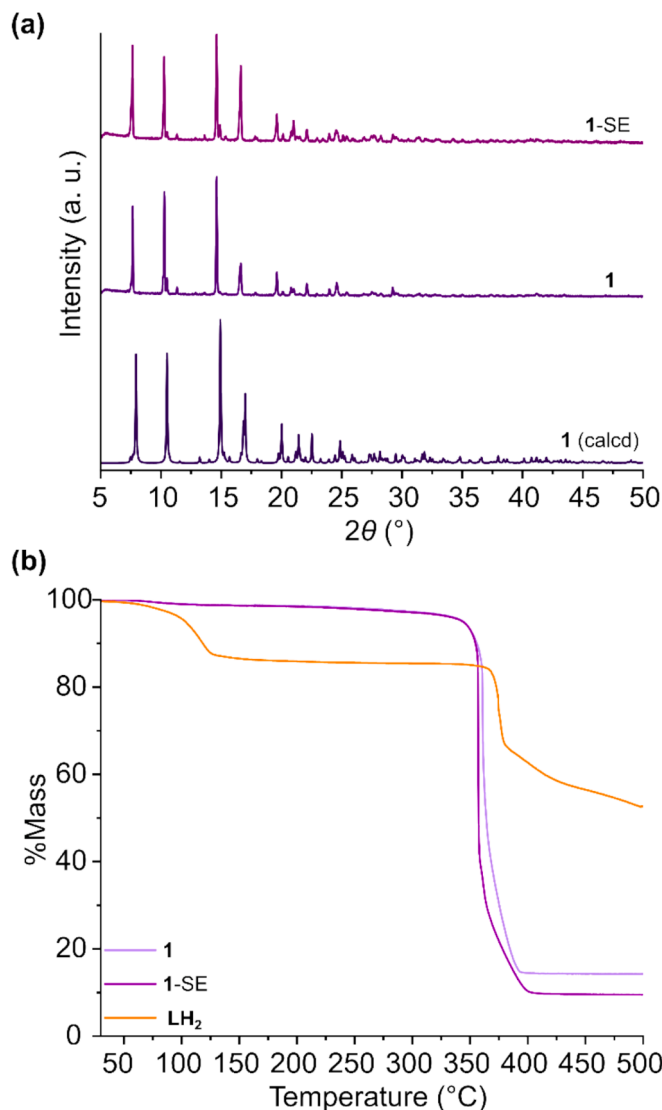

Fig. 5. a) PXRD data for **1** and post-solvent exchange with acetone **1**-SE; b) TGA data for **LH₂** (orange), **1** (dark purple) and **1**-SE (light purple). (For interpretation of the references to colour in this figure legend, the reader is referred to the web version of this article.)

of N_2 at -196 °C (Fig. 6(inset) and Fig. S8). The recorded adsorption isotherm resembles Type II following the IUPAC classification, characteristic of non-porous materials [40]. In this type of isotherm, there is an increase in uptake at high pressures due to multilayer formation and a plateau is not reached. The isotherm also presents a hysteresis Type H3 upon desorption, with the closing of the loop at the cavitation point of the adsorbate, which is between $P/P_0 \approx 0.4$ and 0.5 for N_2 at -196 °C (Fig. S8). This confirms the efficient packing observed in the crystalline structure, and the surface area was found to be negligible. Post-sorption analysis of the sample showed changes in the packing of the molecules, which could be related to the loss of water molecules from the structure during the activation process (Fig. S9).

Before studying gas uptake by **1**, we attempted to exchange the DMA molecules within the structure for a more volatile solvent to facilitate activation [41,42]. For **1** we found that the DMA could not be exchanged – data from attempted exchange with acetone are presented here. The TGA data show a very similar profile to **1** (Fig. 4); the solvent content was found not to have varied by inspection of the acid digested ^{1}H NMR spectra pre- and post-solvent exchange (Fig. S4); and the PXRD data and IR spectra were also found to be invariant (Fig. S5; Fig. S7).

Although these data suggested that removal of the DMA molecules would be difficult, the presence of the bulky NO_2 groups in the spaces between the chains suggested there could be potential gas uptake. This was particularly expected for CO_2, as we anticipated there could be an interaction between the gas and the NO_2 groups [43,44]. **1** displayed minimal uptake of N_2 (Fig. 6(inset); Fig. S10). CO_2 uptake was then measured at 25 °C up to absolute pressures of 20 bar, which is equivalent to $P/P_0 = 0.3$ (Fig. 6). The adsorption isotherm follows a Type I profile without reaching a plateau at the highest pressures measured. The desorption branch shows a hysteresis from 20 bar back to vacuum, where at high pressures the uptake barely diminishes, and when the pressure reaches 4 bar the uptake decreases more markedly (Fig. S11). Overall, the uptake reached at 20 bar is low, with a maxima of 10.7 cm³/ g. The samples from N_2 and CO_2 adsorption were analysed post-sorption using IR, PXRD and ^{1}H NMR (Fig. S5; Fig. S7; Fig. S12; Fig. S13). The NMR data showed that there were no changes in the amount of solvent present within the chains, integrated to 1 DMA molecule per ligand. The IR spectra are in agreement, with no changes in any of the peaks present. PXRD showed no changes in crystalline form or crystallinity, confirming that the Co(II) chains are robust and stable.

4. Conclusions

To summarise, a new semi-rigid ligand, **LH₂**, was synthesised and used to obtain a 1D coordination polymer **1**, that was based on trimeric Co(II) nodes. Based on the crystal structure of the ligand, we had anticipated that it might show permanent porosity, with free volume generated by the bulky elements of the structure, but the uptake of gases was low. The powder X-ray diffraction data for the material pre- and post-gas sorption suggest that a structural rearrangement took place on activation, which might have reduced the potential porosity of the material. Similarly for the polymer **1**, uptake of N_2 was low, while there was modest uptake of CO_2 over the pressure range investigated. We attribute this to the difficulty of removing DMA molecules from the structure, which would have generated significant channels within the polymer – solvent exchange techniques that are commonplace in the study of metal–organic frameworks were unsuccessful here. Nevertheless, we have shown that the new ligand **LH₂** is capable of forming robust coordination polymers.

CRediT authorship contribution statement

Emma Regincós Martí: Writing – review & editing, Writing – original draft, Investigation, Formal analysis. **Jay McCarron:** Writing – review & editing, Investigation. **Beatriz Doñagueda Suso:** Writing – review & editing, Investigation. **Alan R. Kennedy:** Writing – review &
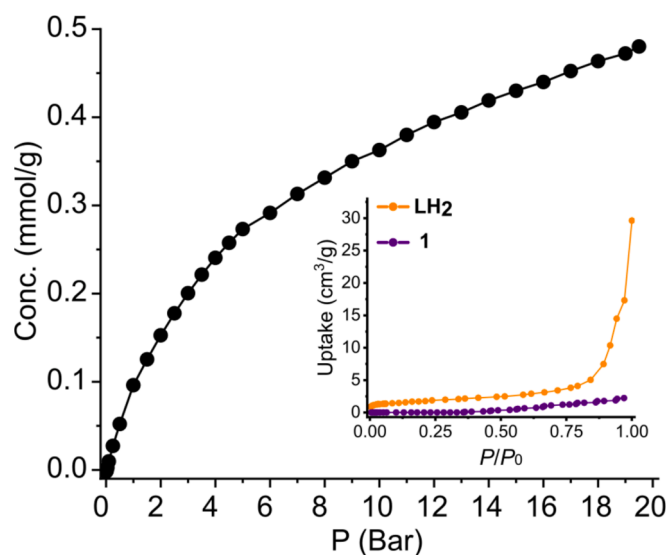

Fig. 6. CO_2 adsorption isotherm for **1**-SE at 25 °C and inset with N_2 adsorption isotherm at -196 °C for **LH₂** (orange) and **1**-SE (purple). (For interpretation of the references to colour in this figure legend, the reader is referred to the web version of this article.)

editing, Formal analysis. **Ashleigh J. Fletcher:** Writing – review & editing, Supervision, Funding acquisition. **Gavin A. Craig:** Writing – review & editing, Writing – original draft, Supervision, Project administration, Funding acquisition, Data curation, Conceptualization.

Declaration of competing interest

The authors declare that they have no known competing financial interests or personal relationships that could have appeared to influence the work reported in this paper.

Appendix A. Supplementary data

CCDC 2378507 and 2378508 contain the supplementary crystallographic data for LH2 and 1. These data can be obtained free of charge via http://www.ccdc.cam.ac.uk/conts/retrieving.html, or from the Cambridge Crystallographic Data Centre, 12 Union Road, Cambridge CB2 1EZ, UK; fax: (+44) 1223-336-033; or e-mail: deposit@ccdc.cam.ac.uk. Supplementary data to this article can be found online at https://doi. org/10.1016/j.poly.2024.117382.

Data availability

The raw data that support the findings of this study are openly available from the University of Strathclyde KnowledgeBase at https:// doi.org/10.15129/45c41c82-c99b-4718-a344-661123e8c211.

References

[1] T. Wang, L. Gao, J. Hou, S.J.A. Herou, J.T. Griffiths, W. Li, J. Dong, S. Gao, M.-M. Titirici, R.V. Kumar, A.K. Cheetham, X. Bao, Q. Fu, S.K. Smoukov, Nat. Commun. 10 (2019) 1340–1349, https://doi.org/10.1038/s41467-019-08972-x.

[2] A. Sur, N.B. Jernigan, D.C. Powers, ACS Catal. 12 (2022) 3858–3867, https://doi.org/10.1021/acscatal.1c05415.

[3] K. Suresh, A.J. Matzger, Angew. Chem. Int. Ed. 58 (2019) 16790–16794, https://doi.org/10.1002/anie.201907652.

[4] P. Horcajada, T. Chalati, C. Serre, B. Gillet, C. Sebrie, T. Baati, J.F. Eubank, D. Heurtaux, P. Clayette, C. Kreuz, J.-S. Chang, Y.K. Hwang, V. Marsaud, P.-N. Bories, L. Cynober, S. Gil, G. Férey, P. Couvreur, R. Gref, Nat. Mater. 9 (2010) 172–178, https://doi.org/10.1038/nmat2608.

[5] X.-L. Qu, B. Yan, Inorg. Chem. 58 (2019) 524–534, https://doi.org/10.1021/acs.inorgchem.8b02738.

[6] Y. Zhang, Y. Liu, F. Huo, B. Zhang, W. Su, X. Yang, A.C.S. Appl, Nano Mater. 5 (2022) 9223–9229, https://doi.org/10.1021/acsanm.2c01556.

[7] N. Hanikel, M.S. Prévot, O.M. Yaghi, Nat. Nanotechnol. 15 (2020) 348–355, https://doi.org/10.1038/s41565-020-0673-x.

[8] W. Liang, P.M. Bhatt, A. Shkurenko, K. Adil, G. Mouchaham, H. Aggarwal, A. Mallick, A. Jamal, Y. Belmabkhout, M. Eddaoudi, Chem 5 (2019) 950–963, https://doi.org/10.1016/j.chempr.2019.02.007.

[9] Y.-Z. Li, G.-D. Wang, L.-N. Ma, L. Hou, Y.-Y. Wang, Z. Zhu, A.C.S. Appl, Mater. Interfaces. 13 (2021) 4102–4109, https://doi.org/10.1021/acsami.0c21554.

[10] Z. Chen, K. Adil, Ł.J. Weseliński, Y. Belmabkhout, M. Eddaoudi, J. Mater. Chem. A 3 (2015) 6276–6281, https://doi.org/10.1039/C4TA07115H.

[11] R. Robson, Chem. Rec. 24 (2024) e202400038, https://doi.org/10.1002/tcr.202400038.

[12] R. Robson, J. Chem. Soc., Dalton Trans. (2000) 3735–3744, https://doi.org/10.1039/B003591M.

[13] B.F. Hoskins, R. Robson, J. Am. Chem. Soc. 112 (1990) 1546–1554, https://doi.org/10.1021/ja00160a038.

[14] D.J. Tranchemontagne, J.L. Mendoza-Cortés, M. O'Keeffe, O.M. Yaghi, Chem. Soc. Rev. 38 (2009) 1257–1283, https://doi.org/10.1039/B817735J.

[15] M.J. Kalmutzki, N. Hanikel, O.M. Yaghi, Sci. Adv., 4 (2018) eaat9180 9181 - 9116. https://doi.org./10.1126/sciadv.aat9180.

[16] D.J. Ashworth, J.A. Foster, J. Mater. Chem. A 6 (2018) 16292–16307, https://doi.org/10.1039/C8TA03159B.

[17] S.R. Batten, N.R. Champness, X.-M. Chen, J. Garcia-Martinez, S. Kitagawa, L. Öhrström, M. O'Keeffe, M.P. Suh, J. Reedijk, Pure Appl. Chem. 85 (2013) 1715–1724, https://doi.org/10.1351/PAC-REC-12-11-20.

[18] S. La Cognata, R. Mobili, C. Milanese, M. Boiocchi, M. Gaboardi, D. Armentano, J.C. Jansen, M. Monteleone, A.R. Antonangelo, M. Carta, V. Amendola, Chem. Eur. J 28 (e202201631) (2022) 202201631, https://doi.org/10.1002/chem.202201631.

[19] Z.-J. Zhang, W. Shi, Z. Niu, H.-H. Li, B. Zhao, P. Cheng, D.-Z. Liao, S.-P. Yan, Chem. Commun. (Camb) 47 (2011) 6425–6427, https://doi.org/10.1039/C1CC00047K.

[20] X.-F. Wang, Y. Chen, L.-P. Song, Z. Fang, J. Zhang, F. Shi, Y.-W. Lin, Y. Sun, Y.-B. Zhang, J. Rocha, Angew. Chem. Int. Ed. 58 (2019) 18808–18812, https://doi.org/10.1002/anie.201909045.

[21] M. Zhu, Z.-M. Hao, X.-Z. Song, X. Meng, S.-N. Zhao, S.-Y. Song, H.-J. Zhang, Chem. Commun. (Camb) 50 (2014) 1912–1914, https://doi.org/10.1039/C3CC48764D.

[22] H. Li, J. Zhou, W. Shi, X. Zhang, Z. Zhang, M. Zhang, P. Cheng, CrstEngComm 16 (2014) 834–841, https://doi.org/10.1039/C3CE41805G.

[23] B. Doñagueda Suso, Z. Wang, A.R. Kennedy, A.J. Fletcher, S. Furukawa, G.A. Craig, Chem. Sci. 15 (2024) 2857–2866, https://doi.org/10.1039/D3SC06140J.

[24] B. Doñagueda Suso, A. Legrand, C. Weetman, A.R. Kennedy, A.J. Fletcher, S. Furukawa, G.A. Craig, Chem. Eur. J., 29 (2023) e202300732 202300731 - 202300739. https://doi.org/10.1002/chem.202300732.

[25] CrysalisPRO, Rigaku Oxford Diffraction Ltd., Yarnton, England, 2016.

[26] G. Sheldrick, Acta Cryst. C 71 (2015) 3–8, https://doi.org/10.1107/S2053229614024218.

[27] L.J. Farrugia, J. Appl. Crystallogr. 45 (2012) 849–854, https://doi.org/10.1107/S0021889812029111.

[28] J. Cirera, P. Alemany, S. Alvarez, Chem. Eur. J. 10 (2004) 190–207, https://doi.org/10.1002/chem.200305074.

[29] S. Alvarez, D. Avnir, M. Llunell, M. Pinsky, New J. Chem. 26 (2002) 996–1009, https://doi.org/10.1039/B200641N.

[30] S.S. Nagarkar, A.K. Chaudhari, S.K. Ghosh, Cryst. Growth Des. 12 (2012) 572–576, https://doi.org/10.1021/cg201630c.

[31] A. Tarushi, X. Totta, C.P. Raptopoulou, V. Psycharis, G. Psomas, D.P. Kessissoglou, Dalton Trans. 41 (2012) 7082–7091, https://doi.org/10.1039/C2DT30547J.

[32] D. Ejarque, T. Calvet, M. Font-Bardia, J. Pons, Molecules 25 (2020) 3615, https://doi.org/10.3390/molecules25163615.

[33] C.-F. Wang, Z.-Y. Zhu, Z.-X. Zhang, Z.-X. Chen, X.-G. Zhou, Cryst. Eng. Comm. 9 (2007) 35–38, https://doi.org/10.1039/B615091H.

[34] S.J. Garibay, J.R. Stork, Z. Wang, S.M. Cohen, S.G. Telfer, Chem. Commun. (2007) 4881–4883, https://doi.org/10.1039/B712118K.

[35] R. Smolková, V. Zeleňák, R. Gyepes, D. Sabolová, N. Imrichová, D. Hudecová, L. Smolko, Polyhedron 141 (2018) 230–238, https://doi.org/10.1016/j.poly.2017.11.052.

[36] R. Smolková, V. Zeleňák, L. Smolko, D. Sabolová, J. Kuchár, R. Gyepes, J. Inorg. Biochem. 177 (2017) 143–158, https://doi.org/10.1016/j.jinorgbio.2017.09.005.

[37] Z. Zhang, Y. Ye, S. Xiang, B. Chen, Acc. Chem. Res. 55 (2022) 3752–3766, https://doi.org/10.1021/acs.accounts.2c00686.

[38] H. Wang, B. Li, H. Wu, T.-L. Hu, Z. Yao, W. Zhou, S. Xiang, B. Chen, J. Am. Chem. Soc. 137 (2015) 9963–9970, https://doi.org/10.1021/jacs.5b05644.

[39] W. Yang, F. Yang, T.-L. Hu, S.C. King, H. Wang, H. Wu, W. Zhou, J.-R. Li, H.D. Arman, B. Chen, Cryst. Growth Des. 16 (2016) 5831–5835, https://doi.org/10.1021/acs.cgd.6b00924.

[40] M. Thommes, K. Kaneko, A.V. Neimark, J.P. Olivier, F. Rodriguez-Reinoso, J. Rouquerol, K.S.W. Sing, Pure Appl. Chem. 87 (2015) 1051–1069, https://doi.org/10.1515/pac-2014-1117.

[41] X. Zhang, Z. Chen, X. Liu, S.L. Hanna, X. Wang, R. Taheri-Ledari, A. Maleki, P. Li, O.K. Farha, Chem. Soc. Rev. 49 (2020) 7406–7427, https://doi.org/10.1039/D0CS00997K.

[42] A.J. Howarth, Y. Liu, P. Li, Z. Li, T.C. Wang, J.T. Hupp, O.K. Farha, Nat. Rev. Mater. 1 (2016) 15018, https://doi.org/10.1038/natrevmats.2015.18.

[43] T.D. Duong, S.A. Sapchenko, I. da Silva, H.G.W. Godfrey, Y. Cheng, L.L. Daemen, P. Manuel, M.D. Frogley, G. Cinque, A.J. Ramirez-Cuesta, S. Yang, M. Schröder, Chem. Sci. 11 (2020) 5339–5346, https://doi.org/10.1039/C9SC04294F.

[44] S. Biswas, T. Ahnfeldt, N. Stock, Inorg. Chem. 50 (2011) 9518–9526, https://doi.org/10.1021/ic201219g.